Biosensors and Bioelectronics 126 (2019) 551–557

Contents lists available at ScienceDirect

Biosensors and Bioelectronics

journal homepage: www.elsevier.com/locate/bios

Rapid, real-time chemiluminescent detection of DNA mutation based on digital microfluidics and pyrosequencing

Fenxiang Zou[a], Qingyu Ruan[a], Xiaoye Lin[a], Mingxia Zhang[a], Yanling Song[b], Leiji Zhou[a], Zhi Zhu[a], Shuichao Lin[a], Wei Wang[b], Chaoyong James Yang[a,b,*]

[a] MOE Key Laboratory of Spectrochemical Analysis & Instrumentation, Collaborative Innovation Center of Chemistry for Energy Materials, Key Laboratory for Chemical Biology of Fujian Province, State Key Laboratory of Physical Chemistry of Solid Surfaces, College of Chemistry and Chemical Engineering, Xiamen University, Xiamen 361005, China

[b] Institute of Molecular Medicine, Renji Hospital, Shanghai Jiao Tong University, School of Medicine, Shanghai 200127, China

ARTICLE INFO

Keywords:
Digital microfluidics
Pyrosequencing
KRAS mutations detection
Gender identification

ABSTRACT

To explore genome mutation meaningfully, it is in urgent need to develop an automated and inexpensive platform for DNA mutation analysis. Digital microfluidics is a powerful platform for a broad range of applications due to the advantages of high automatization and low reagent consumption. Pyrosequencing enables DNA sequencing based on non-electrophoresis bioluminescence, which is suitable for rapid and sensitive analysis of short sequences. Herein, we describe a palmtop sequencing platform for automatic, real-time and portable analysis of DNA mutations, which is based on the pyrosequencing principle and implemented by digital microfluidics. The portable system can sequence a DNA template with up to 53 bp with 100% accuracy within 2 h. Mutation in the KRAS gene can be detected within 30 min with a LOD as low as 5% mutant level. Portable and accurate gender identification was further demonstrated by sequencing a short amelogenin fragment. With the advantages of portability, ease of use, high accuracy, and low cost, the palmtop sequencing platform shows great potential for portable genetic testing in a variety of circumstances.

1. Introduction

DNA mutation analysis is of great importance in many areas, including studies of gene function, discovery of disease-related-marker, and clinical diagnosis. For instance, kirsten rat sarcoma viral oncogene homolog (KRAS) has important effects on cell growth, survival and differentiation, and it is reported that mutations in the KRAS gene is closely related to the development of many cancers (Kranenburg, 2005). For instance, mutations in codons 12 and 13 of the KRAS gene are associated with colorectal carcinomas (Haigis et al., 2008). Detection of the KRAS mutation provides critical information for diagnosis, prognosis and treatment of cancer. Novel approaches for detection of DNA mutations include allele-specific hybridization (Howell et al., 1999), the amplification refractory mutation system (ARMS) (CR et al., 1989), flap endonuclease digestion (Lyamichev et al., 1999), and the high resolution melting (HRM) technique (Audrezet et al., 2008). Although these are useful screening methods, DNA sequencing is still the gold standard for mutation detection, allowing for accurate detection of mutation bases and their locations. However, current sequencing methods rely on complicated systems, with high cost, long processing time, and the need for highly skilled personnel. In addition, the sequencing methods are not well suited for community hospitals, clinics and laboratories due to the high instrumentation costs and complex procedures. As a result, a simple, low-cost, automated, sensitive, and user-friendly sequencing system is highly desirable.

Digital microfluidics (DMF) is an emerging technique to handle discrete picoliter to microliter scale droplets with individually programmed control on patterned electrodes with a hydrophobic surface coating (He et al., 2015; Pollack et al., 2000; Washizu, 1998). Droplets containing samples or reagents can be automatically dispensed, transported, merged, and mixed using a lab-on-a-chip platform. Compared to conventional microfluidics methods (Dou et al., 2016; Li et al., 2018; Shen et al., 2017), DMF offers several advantages in terms of automation, simplicity, flexibility, disposability, and functional integration. Recently, DMF has become a powerful tool for biological and biochemical applications (Jebrail and Wheeler, 2010; Samiei et al., 2016), including enzyme assays (Dou et al., 2016; Nichols and Gardeniers, 2007), immunoassays (Barbulovic-Nad et al., 2008; Miller et al., 2011; Wang et al., 2018), proteomic profiling (Mei et al., 2014; Moon et al., 2006; Wheeler et al., 2004), polymerase chain reactions (Chang et al.,

* Corresponding author at: Institute of Molecular Medicine, Renji Hospital, Shanghai Jiao Tong University, School of Medicine, Shanghai 200127, China.
E-mail address: cyyang@xmu.edu.cn (C.J. Yang).

https://doi.org/10.1016/j.bios.2018.09.092
Received 8 August 2018; Received in revised form 17 September 2018; Accepted 27 September 2018
Available online 02 October 2018
0956-5663/

2006; Hu et al., 2017; Schell et al., 2012), cell-based assays (Aijian and Garrell, 2015; Au et al., 2011; Barbulovic-Nad et al., 2010; Zhou et al., 2007), etc. As a powerful platform for implementing liquid handling steps, DMF eliminates the need for labor-intensive and time-consuming procedures.

Among different sequencing technologies, pyrosequencing is a non-electrophoretic method (Ahmadian et al., 2006; Boles et al., 2011; Ronaghi, 1998; Welch et al., 2011), which is suitable for real-time short sequence analysis with high sensitivity and speed. The pyrosequencing process involves a series of cascade reactions:

$$\mathbf{DNA_n} + \mathrm{dNTP} \xrightarrow{\text{polymerase}} \mathbf{DNA}_{n+1} + \mathrm{PPi} + \mathrm{dNDP} \quad (1)$$

$$\mathrm{PPi} + \mathrm{APS} \xrightarrow{\text{ATP sulfurylase}} \mathrm{ATP} + \mathbf{SO_4^{2-}} \quad (2)$$

$$\mathrm{ATP} + \mathbf{O_2} + \mathrm{luciferin} \xrightarrow{\text{luciferase}} \mathrm{AMP} + \mathrm{PPi} + \mathbf{CO_2} + \mathrm{oxyluciferase} + \mathrm{light} \quad (3)$$

(1) With the addition of the necessary dNTPs and polymerase, the DNA template (DNA_n) elongates with the help of polymerase, releasing pyrophosphate (PPi). (2) In the presence of adenosine phosphosulfate (APS) and ATP sulfurylase, PPi is converted to ATP, which allows (3) the oxidation of luciferin, catalyzed by luciferase and subsequent generation of light for detection. Since the pyrosequencing process consists of a series of liquid handling steps, it is highly amenable to using DMF for automated sequencing.

In this work, we report a Palmtop Pyrosequencer for the detection of gene mutations. The system is based on digital microfluidics to automatically sequence DNA by pyrosequencing at the plain hydrophobic surface of a printed-circuit board (PCB). The reaction of pyrosequencing can be programmed control automatically, making the sequencing instrument much simpler, and allowing rapid and real-time mutation analysis. Considering that the low cost and customizability of the platform, a series of applications can be potentially implemented, such as DNA methylation analysis and bacterial strain typing.

2. Experimental

2.1. Reagents and apparatus

All chemicals were obtained from commercial sources and used without further purification. Easy Taq DNA Polymerase was purchased from Trans Biotech (Beijing, China). Deoxynucleotides (dNTPs), DNA polymerase Klenow fragment and Dynabeads™ M-280 streptavidin were purchased from Thermo Fisher Scientific (Waltham, MA, USA). Adenosine 5′-phosphosulfate (APS), D-luciferin and inorganic pyrophosphatase (PPase) were obtained from Sigma-Aldrich (St. Louis, MO, USA). Luciferase and single-stranded binding protein (SSB) were purchased from Molecular Cloning Laboratories (MCLAB). ATP sulfurylase was obtained from New England BioLabs (NEB). Sodium 2′-deoxyadenosine 5′-O-(1-triphosphate) (dATP-α-S) was obtained from Amersham Pharmacia Biotech (Amersham, UK). Teflon AF was purchased from Dupont (China).

The buffer solutions used were as follow: Binding buffer contained 10 mM tris buffer (pH 7.6), 2 M NaCl, 1 mM EDTA (pH 7.6) and 0.1% Tween 20; Magnesium annealing buffer contained 20 mM tris acetate (pH 7.6) and 5 mM magnesium acetate; Washing buffer contained 100 mM tris acetate (pH 7.6), 0.5 mM ethylenediaminetetraacetic acid (EDTA, pH 8.0), 5 mM magnesium acetate, and 0.01% Tween 20. All solutions were prepared with water (resistivity of 18 MΩ/cm) from a purification system. The template and primers were used in the work are designed as Supporting information (Supporting information, Table S1), all were synthesized by Sangon Biotech (Shanghai). PCR amplification was run on Alpha™ Unit Block Assembly for DNA Engine Systems (Albuquerque, Mexico, USA).

2.2. Extraction of genomic DNA

Genomic DNA was obtained from cell lines, oral epithelium cells, and colon carcinoma tissue by using the TIANamp Genomic DNA kit (Tiangen Biotech, Beijing, China). Purifed DNA was eluted with 50 μL of elution buffer and stored at − 20 ℃. Cell lines include HeLa (human cervix cancer cell), SW480 (human colon cancer cell) and LoVo (human colon cancer cell), which were obtained from the American Type Culture Collection (ATCC). Both HeLa and SW480 lines were cultured in Dulbecco's minimal essential medium (Hyclone) with 10% fetal bovine serum (FBS, Invitrogen); LoVo was cultured in RPMI 1640 media, at 37 ℃ in a humidified atmosphere of 5% CO_2 and 95% air. Oral epithelium cells were provided by normal volunteers of Xiamen University. And the Colon carcinoma tissue samples were obtained from the PLA 174th hospital. Including 4 from patients and 1 from normal (Supporting information, Table S2). Whole tissue samples were collected without preservatives and stored at − 80 ℃. The tissue sample providers have been given informed consent for the experiments. The study protocols were based on the ethical principles for research that involves human subjects of the Helsinki Declaration for medical research37 and technical guidelines for clinical trials of in vitro diagnosis (issued by China Food and Drug Administration/2014/No. 16).

2.3. Amplifications assay

In the mutation assay, the oligonucleotides Kras forward primer and Kras reverse primer (Table S1) were used as forward and reverse primers, respectively. PCR reactions were performed in a total volume of 50 μL containing 1–30 ng of genomic DNA (extract from three cell lines and tissue samples), 1 × Taq buffer, 200 μM of each dNTP, 0.4 μM of each primer set and 2.5 U of Taq DNA polymerase. The amplification procedure (94 ℃ for 30 s, 60 ℃ for 30 s, and 72 ℃ for 30 s) were performed for 25 cycles.

In the gender identification study, the oligonucleotides AMEL forward primer and AMEL reverse primer (Table S1) were used as forward and reverse primers, respectively. PCR reactions were performed as described above. And the amplification procedure (95 ℃ for 15 s, 50 ℃ for 30 s, and 72 for 15 s) were performed for 25 cycles.

2.4. Sample preparation

The biotinylated PCR products were mixed with 30 μL streptavidin M280 Dynabeads and 20 μL binding buffer, and incubated at room temperature using a shaker for 30 min. The non-biotinylated strands were removed using 100 μL of 0.1 M NaOH. Then washed three times with magnesium annealing buffer, the template-beads were released in annealing buffer with 50 pmol sequencing primer. The mixture was heated at 80 ℃ for 2 min and cooled to room temperature to allow the sequencing primer and template DNA to anneal. Then the template-primer-beads were washed three times with washing buffer and re-suspended in 100 μL of washing buffer. About 12 μg of single-stranded binding protein (SSB) was added, and the mixture was incubated at room temperature for 10 min. The beads were washed with washing buffer and resuspended in 60 μL of pyrosequencing washing buffer to achieve a final concentration of 5 μg beads/μL.

2.5. Design and fabrication of digital microfluidic chip

The digital microfluidic chip contained a bottom plate and a top plate. The bottom substrate electrode (65.2 mm × 47.1 mm, 1.6 mm thickness) was fabricated from printed circuit board (PCB) and the design featured an array of 40 actuation electrodes connected to 8 reservoir electrodes, with interelectrode gaps of 10 μm. Then the bottom plate was coated with a layer of Parylene C dielectric (8 μm) by vapor deposition as a dieletric layer to insulate electrodes and droplets, and then spin-coated with a layer of Teflon AF (100 nm, 60 s, 1500 rpm),

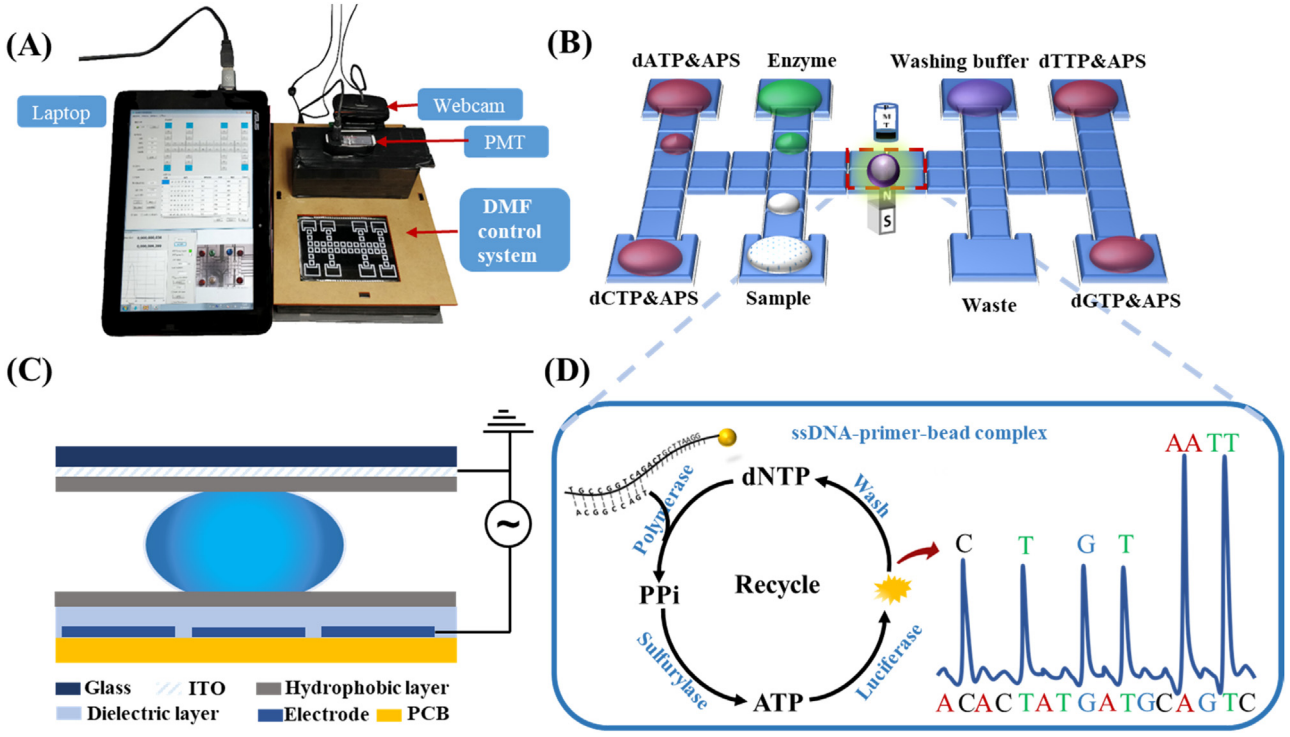

Fig. 1. (A) Photograph of the Palmtop Pyrosequencer. (B) Schematic illustration of the reaction chip, including multiplex reservoirs and a detection zone. (C) Schematic of cross section through the electrode array. (D) Working principle of pyrosequencing.

followed by baking on a hot plate (160 °C, 15 min). DMF top plates were formed from indium tin oxide (ITO) coated glass, which was spin-coated with Teflon-AF (100 nm, 60 s, 1500 rpm) and baked on a hot plate (160 °C, 15 min). The top and bottom plates are separated by about 125 μm thick single-sided tape (Scotch Brand) and filled with fluorocarbon oil (FC 40). The volume of the unit actuation electrode and reservoir electrode droplet were about 1 and 10 μL, respectively.

2.6. Palmtop pyrosequencer platform

The Photograph of the Palmtop Pyrosequencer is displayed in Fig. 1(A). The Palmtop Pyrosequencer platform approximate dimensions 25 × 18 × 8 cm (l × w × h), which is as small as a tablet computer. And it contained four principal parts: EWOD system (electrowetting-on-dielectric), webcam, laptop, and an integrated photon-counting photomultiplier tube (PMT, H11890, Hamamatsu, Japan). The cost of all instrumental parts is about $3000 with the PMT being the most expensive part. The EWOD system consisted of a DMF control system, microfluidic software, DMF chip and a magnet. The chip was positioned on a custom-built acrylic board, which was connected to the DMF control system via a PCI-E pin interface (64 pins). A magnet was placed under the chip to separate the beads. Droplet manipulation was driven by applying sine wave potentials (150–180 Vrms, 10 kHz) between the top plate reference electrode and the electrodes on the PCB surface. All basic liquid handling operations, such as merging, mixing, moving and splitting could be performed accurately and reliably by the software, monitored and recorded by a webcam (Video S1 & S2). The chemiluminescence signal is measured by the integrated PMT, and recorded by a laptop.

Supplementary material related to this article can be found online at doi:10.1016/j.bios.2018.09.092.

3. Results and discussion

3.1. Working principle of the palmtop pyrosequencer

The Photograph of the Palmtop Pyrosequencer is displayed as Fig. 1(A). The DMF Chip is designed with 8 reservoir electrodes to loading reagents and 40 actuation electrodes to control the droplets (Fig. 1(B)). The washing buffer, enzymes (polymerase, sulfurylase, luciferase), 4 types of dNTPs, APS, and the sample (single-stranded target DNA immobilized on magnetic particles) are placed in seven reservoirs, respectively. Fig. 1(C) shows the schematic of a cross section through the electrode array. And Fig. 1(D) shows the working principle of pyrosequencing, which was conducted by DMF. Each round of nucleotide addition reaction is performed according to the following steps: (1) A sample droplet (~ 2 μL) is dispensed from the reservoir, then transported to the detection zone. (2) The magnet beneath the chip is engaged, and the beads are immobilized while the supernatant is driven to the waste reservoir. (3) The droplets of one kind of dNTP and enzymes are dispensed to resuspend the beads. The resulting droplet is then mixed fully by transporting it back and forth across eight electrodes and moved to the detection zone, where chemiluminescence is measured by the integrated photomultiplier (PMT) for 1 min (4) After detection, step 2 is repeated. (5) A droplet of washing buffer is driven to the immobilized beads, the magnet is then disengaged, and the droplet is mixed to resuspend the beads followed by a repeat of step 2. (6) Step 5 is repeated three times, and then followed by the next round of nucleotide addition. For de novo sequencing, each dNTP addition is programmed from step 3–6, in turn. The complete protocol for the pyrosequencing on DMF is displayed in Video S3. Every nucleotide addition cycle takes approximately 3.5 min, including sample loading (30 s), reagent mixing (30 s), signal detection (60 s), bead collection (30 s) and washing (60 s).

Supplementary material related to this article can be found online at doi:10.1016/j.bios.2018.09.092.

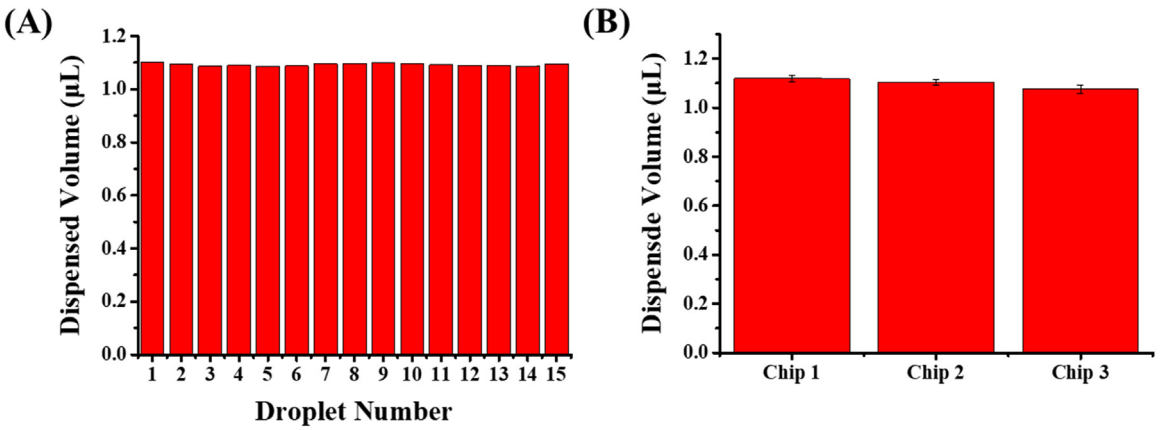

Fig. 2. (A) Volume of 15 droplets dispensed from the same reservoir. (B) Plot showing the average volume of 15 dispensed droplets from three chips.

3.2. Droplet dispensing on the DMF device

Since batch effects of droplet volumes would influence the detection result, the uniformity of the dispensed droplet volumes was first evaluated. The uniformity and accuracy of droplet dispensing depend on several factors, such as the sizes of the reservoirs and electrodes, the viscosity of the droplet, and the actuation voltage of the device. When the gap of the two parallel plates is fixed, the droplets volume depends on area. Firstly, the volume of droplets dispensed from the reservoir electrode were measured. The droplets were imaged with a CCD camera and the Nano Measurer software was used to estimate the apparent cross-sectional area of each droplet and volume (knowing the spacer thickness). As shown in Fig. 2(A), fifteen droplets were dispensed from the same reservoir, and the coefficients of variation (CV) in 15 dispensed volumes was 0.4%, which was better than other reported DMF devices (Eydelnant et al., 2012; Fouillet et al., 2007). Fouillet et al. reported a CV of about 4% for droplet dispensing of reagent into oil-filled DMF devices. And Eydelnant et al. demonstrate the CVs of 0.7–13.8% with dispensing of volumes ranging from 80 to 800 nL. In our device, the batch-to-batch variation was 1.9% by measuring three chips [Fig. 2(B)], which was better than that achieved by manual pipetting. For example, manual dispensing of a 1 μL droplet using a 0.2–2.0 μL pipette resulted in a typical CV of 4.0%. These results demonstrated the accuracy and reliability of the DMF system for liquid handling. Instead of the usual manual pipetting, the DMF system enables automated and programmed manipulation, reducing the operational complexity, volume variation, and labor cost.

3.3. Characterization of washing efficiency

Since the amounts of reagent leftovers will influence the final result, it is important to remove extra dNTPs and other reagents completely. The single-stranded target DNA immobilized on magnetic particles is concentrated by a permanent magnet under the detection zone and washed with fresh washing droplets, then the supernatant is transferred to the waste reservoir. A sequence of images illustrating a wash cycle is shown in Fig. S1. To verify the washing efficiency of the digital microfluidics system, the chemiluminescence signal was measured after a certain nucleotide (dCTP) was incorporated and the beads were washed with different numbers of cycles. As shown in Fig. 3(A), the chemiluminescence signal was equivalent to background after just two wash cycles, relatively to six wash cycles in a 96-well plate. Therefore, we washed twice after each nucleotide was incorporated in subsequent experiments. As shown in Fig. 3(B), when there was no washing, the signal generated from template elongation decayed over time, taking about 150 min to reach background intensity. This result indicated that the signal reduction in Fig. 3(A) resulted from washing, rather than natural signal decay. Overall, the DMF system enabled complete and efficient washing during the pyrosequencing.

3.4. Feasibility of re-sequencing and de novo sequencing

To achieve high performance, the concentrations of APS/D-luciferin/dNTPs and the number of PCR cycles were first optimized (Fig. S2 & S3). In pyrosequencing, the signal intensity is related to the corresponding incorporated base numbers. To establish a quantitative relationship between the signal intensity and the number of incorporated nucleotides, multiple dNTP (one, two, or three different nucleotides) were mixed simultaneously in dNTPs solution. Then the solution was added to prime DNA templates, and the peaks obtained by the corresponding dNTP addition were associated with the number of bases. As shown in Fig. 4A, a linear relationship was obtained with the increasing

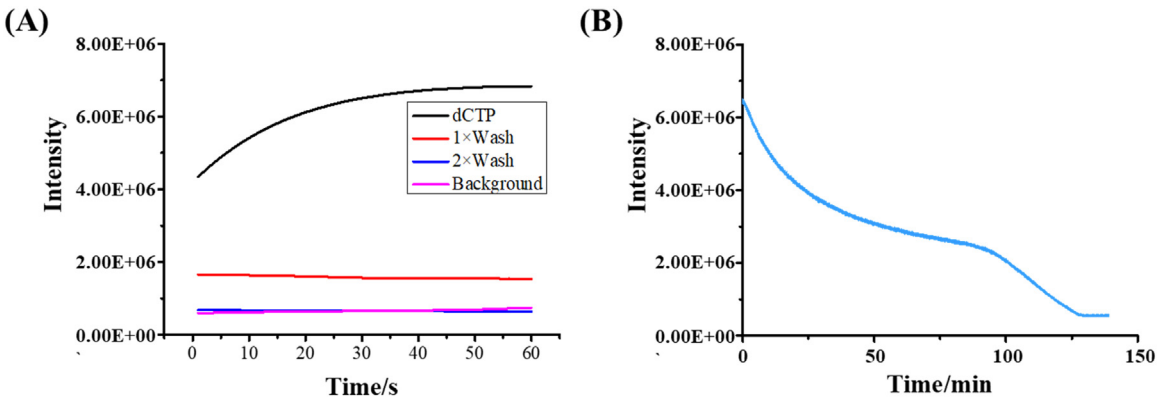

Fig. 3. (A) After dCTP incorporation, residual signal was determined during each wash cycle. (B) Natural decay of the resulting luminescence.

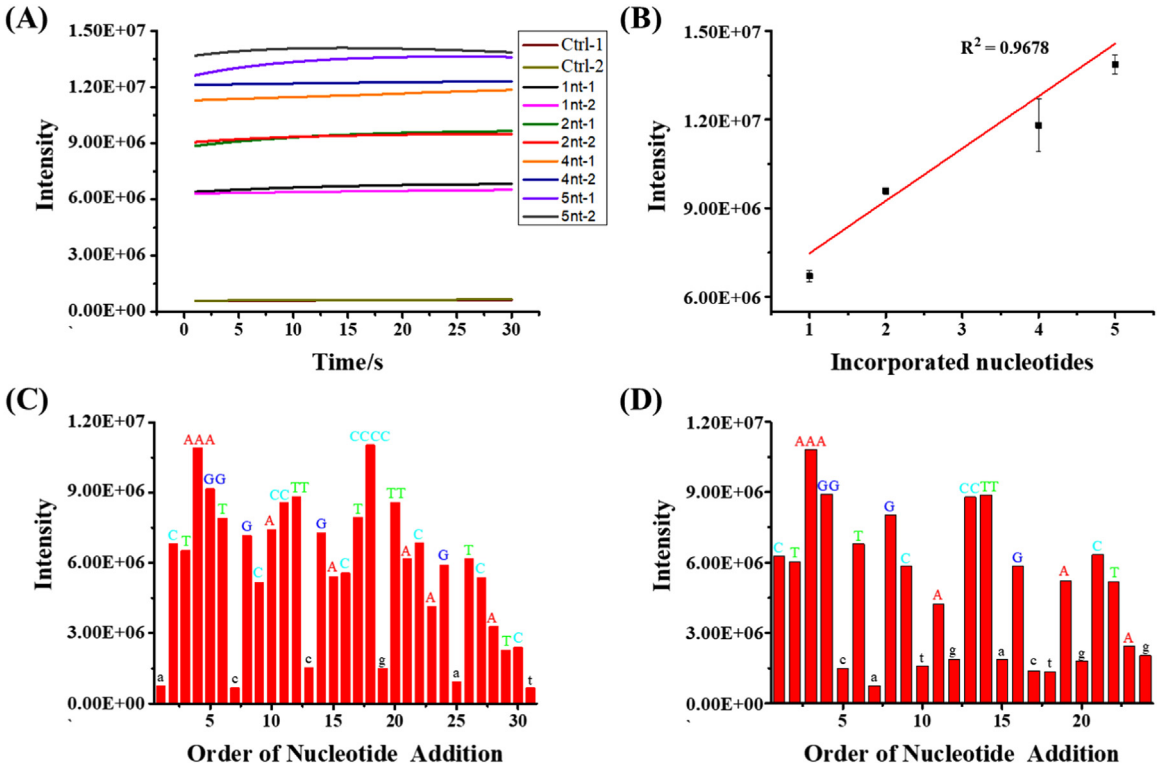

Fig. 4. (A) Relationship between signal intensity and the corresponding number of incorporated bases in one peak (in duplicate). (B) Linearity of the luminescence signal with respect to the number of nucleotides incorporated. (C) Histograms of re-sequence. (D) Histograms of de novo pyrosequencing.

numbers of incorporated nucleotides [R^2 = 0.97, Fig. 4(B)]. Therefore, different numbers of incorporated base numbers can be distinguished by our Palmtop Pyrosequencer.

Then we used the device for re-sequencing and de novo sequencing. In re-sequencing, dNTPs were added in a corresponding order based on the template sequence, and the background signal was determined by incorporating mismatched nucleotides. As shown in Fig. 4(C), the sequence could be obtained directly from the histogram, which showed that the sequence of 34 bases was read within 30 reactions with 100% accuracy, resulting in a read length of 53 bp considering the 19 bp primer. For de novo sequencing, four kinds of nucleotides were typically added periodically, such as CTAG-CTAG···. We performed additions of four nucleotides in a repeated cyclical fashion (6 cycles), resulting in a 19-base read [Fig. 4(D)]. The experimentally determined

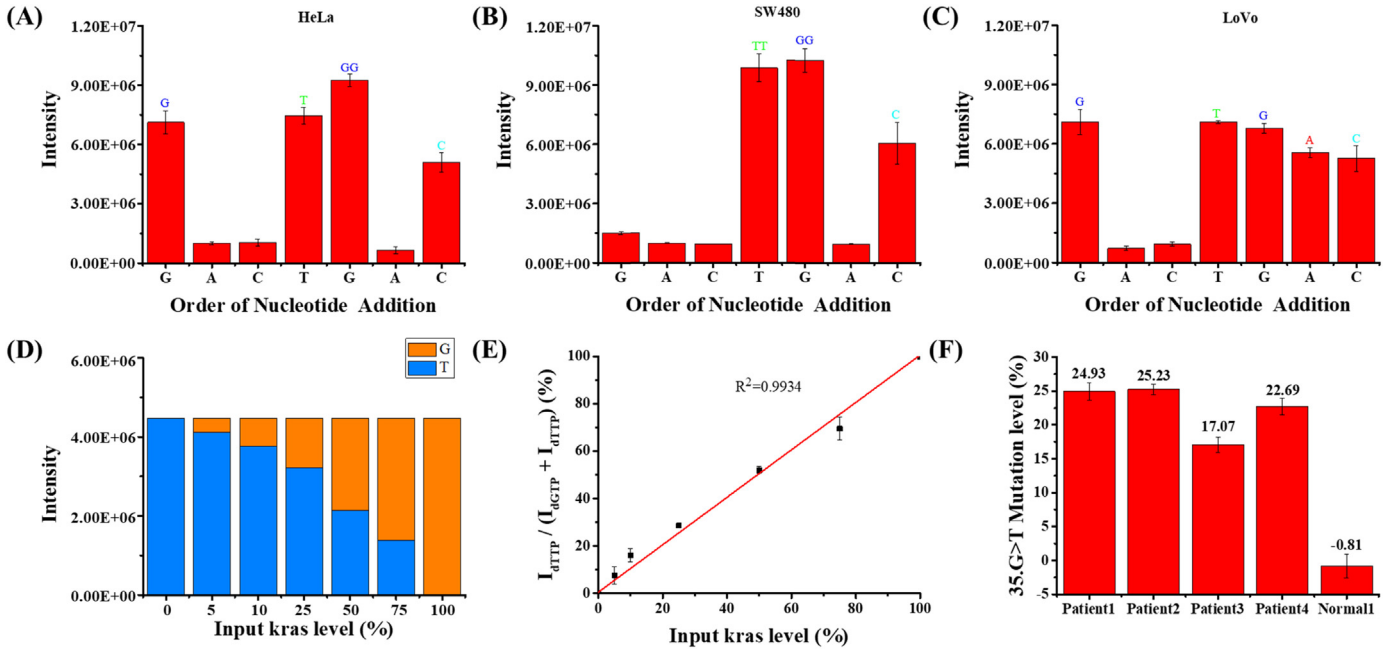

Fig. 5. (A, B, C) Chemiluminescence signal responses of Palmtop Pyrosequencer to DNA from different cells. (A) Hela (GTGGC), (B) SW480 (TTGGC) and (C) LoVo (GTGAC). (D) Histogram showing the signal responses of G/T in different mutant levels of c. 35G > T. (E) Calibration curve for the various levels of input mutation. (F) Clinical assay performance of DNA extracted from colon carcinoma tissues of four patient samples and one normal sample.

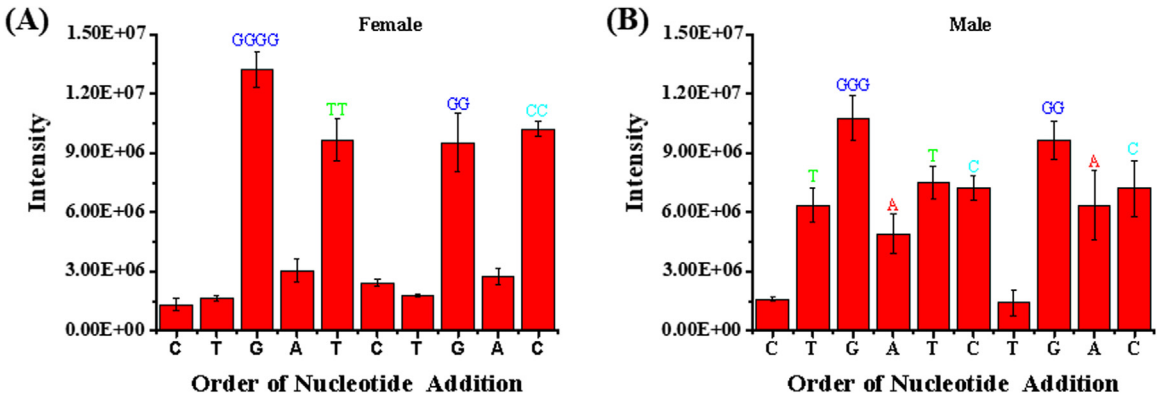

Fig. 6. Chemiluminescence signal responses of Palmtop Pyrosequencer to DNA from females and males (A) Histogram of female (GGGGTTGGCC) and (B) male (TGGGATCGGAC).

sequence read directly from the data was 100% accurate. For both re-sequencing and de novo sequencing, the chemiluminescence signal intensity decay is inevitable, especially after 25 cycle reactions, which is mainly due to the loss of the DNA template during the washing process and imperfect reactions. Nonetheless, the correspondence between signal intensity and incorporated base numbers could be preserved before 25 cycle reactions, thus meeting the requirement for analysis of mutations. Therefore, these results clearly showed that the system can be used to analyze gene mutation for short sequences.

3.5. KRAS mutation detection

After demonstrating the feasibility, we applied the system for detection of KRAS mutation. First, we validated the possibility of mutation detection in cultured cell samples. DNA was extracted from three cell lines: SW480 with the KRAS mutation c.35G > T (codon 12 GGT > GTT), LoVo with the c.38G > A mutation (codon 13 GGC > GAC), and HeLa with wild-type KRAS (Ogino et al., 2005). The design of mutation detection is shown in Fig. S4, and the sequencing primer was designed to hybridize with the template in front of the mutation site. The nucleotides were dispersed in an order of GACTGAC, and the sequence results of wild-type and mutant KRAS are shown in Fig. 5(A)-(C), with a readout of GTGGC for HeLa, TTGGC for SW480 and GTGAC for LoVo. The results showed that the SW480 cell at codon 12 was detected with mutation c.35G > T (codon 12 GTT), and the LoVo cell at the codon 13 was also detected with mutation c.38G > A (codon 13 GAC), all of which were consistent with the literature. We further evaluated the performance of the system for detecting different levels of mutation. We mixed the DNA template of KRAS-mutant and KRAS-wild type (codon 12 (c.35G > T)) in different ratios (0%, 5%, 10%, 25%, 50%, 75%, and 100%) and then sequenced them using our system. Fig. 5(D) showed the signal responses (after background correction) of G/T in different mutant levels of c.35 G > T. Then according to the equation of $E = I_{mutant}/(I_{mutant} + I_{wild\text{-}type})$, mutant levels corresponding to input levels were obtained with correlation coefficient of 0.99 (Fig. 5(E)). Notably, the 5% mutation could be clearly identified, which will be useful for tumors containing abundant non-neoplastic cells (Ogino et al., 2005). These results demonstrated that our Palmtop Pyrosequencer was capable of accurately quantifying the mutation levels. According to the calibration curve of $I_{dTTP}/(I_{dGTP} + I_{dTTP})$, we explored the mutation of codon 12 (c.35G > T) for colon carcinoma tissue and normal tissue. As shown in Fig. 5(F), all four patient samples produced higher signals than the normal sample. In the four patient samples, the mutation levels of codon 12 (c.35G > T) were estimated as about 20%, while the normal sample was 0%, which is consistent with the reported literature (Heinemann et al., 2009). These results revealed that our platform can be applied to detect KRAS mutation in tumor. Moreover, our platform was also capable of quantifying the level of mutations, which is important for cancer diagnosis, evaluation of efficacy of anti-tumor drugs, and monitoring tumor prognosis.

3.6. Gender identification

To demonstrate the versatility, we applied the Palmtop Pyrosequencer for gender identification by sequencing a short amelogenin (AMEL) fragment. Reliable identification of gender is important in forensic science and clinical research. Numerous polymorphisms on the gender identification are presented on the two homologous copies of the amelogenin gene on the X and Y chromosomes (AMELX/AMELY) (Tschentscher et al., 2008). Cong et al. (Li et al., 2012) showed that a 44/45 bp fragment of the human amelogenin gene with three single nucleotide polymorphism loci and an index motif on chromosomes X and Y widely existed (Fig. S6). We used the Palmtop Pyrosequencer to analyze the sequence for gender identification within 30 min. Genome DNA extraction of oral epithelial cells from 10 volunteers (5 males and 5 females) were analyzed by the Palmtop Pyrosequencer. As shown in Fig. 6(A) and (B) the nucleotide was dispensed as CTGATCTGAC, and the readouts were GGGGTTGGCC for female samples and TGGGATCG GAC for male samples, which is consistent with the reported literature (Li et al., 2012). Gender information for all 10 samples was correctly determined. These results clearly demonstrated that our platform could be used for SNP genotyping.

4. Conclusions

In conclusion, a Palmtop Pyrosequencer based on digital microfluidics was successfully developed for gene mutation detection. The system consists of 48 electrodes for digital microfluidic control, a PMT module for the chemiluminescent signal readout, and a circular magnet assembly for the manipulation of particles. Compared to commercial instruments, the system offers significant advantages in terms of instrument size, easy operation, high sensitivity, and low cost. Additionally, the reliable detection of KRAS mutation in 5 real patients' samples have validated the potential for use in community hospitals, clinics and laboratories for different genetic analyses. Furthermore, the Palmtop Pyrosequencer system is highly applicable as a protable platform for various applications, including SNP genotyping, bacterial strain typing, mutation detection in tumors, and quantitative CpG island methylation analysis. Now, several samples cannot be detected simultaneously due to the chip design. In future, with improvements in microfluidic design, it is expected that longer reads, higher throughput, and improved process integration can be achieved.

Acknowledgements

We thank the National Natural Science Foundation of China (21735004, 21435004, 21775128, 21521004, 21705024, 21874089), and Program for Changjiang Scholars and Innovative Research Teams in University (IRT13036) for their financial support.

Appendix A. Supplementary material

Supplementary data associated with this article can be found in the online version at doi:10.1016/j.bios.2018.09.092

References

Ahmadian, A., Ehn, M., Hober, S., 2006. Pyrosequencing: history, biochemistry and future. Clin. Chim. Acta 363 (1–2), 83–94.
Aijian, A.P., Garrell, R.L., 2015. Digital microfluidics for automated hanging drop cell spheroid culture. J. Lab. Autom. 20 (3), 283–295.
Au, S.H., Shih, S.C., Wheeler, A.R., 2011. Integrated microbioreactor for culture and analysis of bacteria, algae and yeast. Biomed. Microdevices 13 (1), 41–50.
Audrezet, M.P., Dabricot, A., Le Marechal, C., Ferec, C., 2008. Validation of high-resolution DNA melting analysis for mutation scanning of the cystic fibrosis transmembrane conductance regulator (CFTR) gene. J. Mol. Diagn. 10 (5), 424–434.
Barbulovic-Nad, I., Yang, H., Park, P.S., Wheeler, A.R., 2008. Digital microfluidics for cell-based assays. Lab Chip 8 (4), 519–526.
Barbulovic-Nad, I., Au, S.H., Wheeler, A.R., 2010. A microfluidic platform for complete mammalian cell culture. Lab Chip 10 (12), 1536–1542.
Boles, D.J., Benton, J.L., Siew, G.J., Levy, M.H., Thwar, P.K., Sandahl, M.A., Rouse, J.L., Perkins, L.C., Sudarsan, A.P., Jalili, R., Pamula, V.K., Srinivasan, V., Fair, R.B., Griffin, P.B., Eckhardt, A.E., Pollack, M.G., 2011. Droplet-based pyrosequencing using digital microfluidics. Anal. Chem. 83 (22), 8439–8447.
Chang, Y.H., Lee, G.B., Huang, F.C., Chen, Y.Y., Lin, J.L., 2006. Integrated polymerase chain reaction chips utilizing digital microfluidics. Biomed. Microdevices 8 (3), 215–225.
Dou, M., Garcia Jr., J.M., Zhan, S., Li, X., 2016. Interfacial nano-biosensing in microfluidic droplets for high-sensitivity detection of low-solubility molecules. Chem. Commun. 52 (17), 3470–3473.
Eydelnant, I.A., Uddayasankar, U., Li, B., Liao, M.W., Wheeler, A.R., 2012. Virtual microwells for digital microfluidic reagent dispensing and cell culture. Lab Chip 12 (4), 750–757.
Fouillet, Y., Jary, D., Chabrol, C., Claustre, P., Peponnet, C., 2007. Digital microfluidic design and optimization of classic and new fluidic functions for lab on a chip systems. Microfluid Nanofluidics 4 (3), 159–165.
Haigis, K.M., Kendall, K.R., Wang, Y., Cheung, A., Haigis, M.C., Glickman, J.N., Niwa-Kawakita, M., Sweet-Cordero, A., Sebolt-Leopold, J., Shannon, K.M., Settleman, J., Giovannini, M., Jacks, T., 2008. Differential effects of oncogenic K-Ras and N-Ras on proliferation, differentiation and tumor progression in the colon. Nat. Genet. 40 (5), 600–608.
He, J.L., Chen, A.T., Lee, J.H., Fan, S.K., 2015. Digital microfluidics for manipulation and analysis of a single cell. Int. J. Mol. Sci. 16 (9), 22319–22332.
Heinemann, V., Stintzing, S., Kirchner, T., Boeck, S., Jung, A., 2009. Clinical relevance of EGFR- and KRAS-status in colorectal cancer patients treated with monoclonal antibodies directed against the EGFR. Cancer Treat. Rev. 35 (3), 262–271.
Howell, W.M., Jobs, M., Gyllensten, U., Brookes, A.J., 1999. Dynamic allele-specific hybridization. Nat. Biotechnol. 17, 87–88.
Hu, C., Kalsi, S., Zeimpekis, I., Sun, K., Ashburn, P., Turner, C., Sutton, J.M., Morgan, H., 2017. Ultra-fast electronic detection of antimicrobial resistance genes using isothermal amplification and Thin Film Transistor sensors. Biosens. Bioelectron. 96, 281–287.
Jebrail, M.J., Wheeler, A.R., 2010. Let's get digital: digitizing chemical biology with microfluidics. Curr. Opin. Chem. Biol. 14 (5), 574–581.
Kranenburg, O., 2005. The KRAS oncogene: past, present, and future. Biochim. Biophys. Acta 1756 (2), 81–82.
Li, S., Feng, T., Fu, L., Li, Z., Lou, C., Zhang, X., Ma, C., Cong, B., 2012. Pyrosequencing of a short fragment of the amelogenin gene for gender identification. Mol. Biol. Rep. 39 (6), 6949–6957.
Li, X., Zhang, D., Zhang, H., Guan, Z., Song, Y., Liu, R., Zhu, Z., Yang, C., 2018. Microwell array method for rapid generation of uniform agarose droplets and beads for single molecule analysis. Anal. Chem. 90 (4), 2570–2577.
Lyamichev, V., Mast, A.L., Hall, J.G., Prudent, J.R., Kaiser, M.W., Takova, T., Kwiatkowski, R.W., Sander, T.J., de Arruda, M., Arco, D.A., Neri, B.P., Brow, M.A., 1999. Polymorphism identification and quantitative detection of genomic DNA by invasive cleavage of oligonucleotide probes. Nat. Biotechnol. 17 (3), 292–296.
Mei, N., Seale, B., Ng, A.H., Wheeler, A.R., Oleschuk, R., 2014. Digital microfluidic platform for human plasma protein depletion. Anal. Chem. 86 (16), 8466–8472.
Miller, E.M., Ng, A.H., Uddayasankar, U., Wheeler, A.R., 2011. A digital microfluidic approach to heterogeneous immunoassays. Anal. Bioanal. Chem. 399 (1), 337–345.
Moon, H., Wheeler, A.R., Garrell, R.L., Loo, J.A., Kim, C.J., 2006. An integrated digital microfluidic chip for multiplexed proteomic sample preparation and analysis by MALDI-MS. Lab Chip 6 (9), 1213–1219.
Newton, C.R., Graham, A., Heptinstall, L.E., Powell, S.J., Summers, C., Kalsheker, N., Smith, J.C., Markham, A.F., 1989. Analysis of any point mutation in DNA. The amplification refractory mutation system (ARMS). Nucleic Acids Res. 17 (7).
Nichols, K., Gardeniers, H., 2007. A digital microfluidic system for the investigation of pre-steady-state enzyme kinetics using rapid quenching with MALDI-TOF mass spectrometry. Anal. Chem. 79 (22), 8699–8704.
Ogino, S., Kawasaki, T., Brahmandam, M., Yan, L., Cantor, M., Namgyal, C., Mino-Kenudson, M., Lauwers, G.Y., Loda, M., Fuchs, C.S., 2005. Sensitive sequencing method for KRAS mutation detection by pyrosequencing. J. Mol. Diagn. 7 (3), 413–421.
Pollack, M.G., Fair, R.B., Shenderov, A.D., 2000. Electrowetting-based actuation of liquid droplets for microfluidic applications. Appl. Phys. Lett. 77 (11), 1725–1726.
Ronaghi, M., 1998. DNA sequencing:a sequencing method based on real-time pyrophosphate. Science 281 (5375), 363–365.
Samiei, E., Tabrizian, M., Hoorfar, M., 2016. A Review of Digital Microfluidics as Portable Platforms for Lab-on a-chip Applications.
Schell, W.A., Benton, J.L., Smith, P.B., Poore, M., Rouse, J.L., Boles, D.J., Johnson, M.D., Alexander, B.D., Pamula, V.K., Eckhardt, A.E., Pollack, M.G., Benjamin Jr., D.K., Perfect, J.R., Mitchell, T.G., 2012. Evaluation of a digital microfluidic real-time PCR platform to detect DNA of Candida albicans in blood. Eur. J. Clin. Microbiol. Infect. Dis. 31 (9), 2237–2245.
Shen, F., Li, Y., Liu, Z., Li, X., 2017. Study of flow behaviors of droplet merging and splitting in microchannels using Micro-PIV measurement. Microfluid Nanofluidics 21, 4.
Tschentscher, F., Frey, U.H., Bajanowski, T., 2008. Amelogenin sex determination by pyrosequencing of short PCR products. Int. J. Leg. Med. 122 (4), 333–335.
Wang, Y., Ruan, Q., Lei, Z.-C., Lin, S.-C., Zhu, Z., Zhou, L., Yang, C., 2018. Highly sensitive and automated surface enhanced Raman scattering-based immunoassay for H5N1 detection with digital microfluidics. Anal. Chem. 90 (8), 5224–5231.
Washizu, M., 1998. Electrostatic actuation of liquid droplets for microreactor applications. IEEE Trans. Ind. Appl. 34 (4), 732–737.
Welch, E.R., Lin, Y.Y., Madison, A., Fair, R.B., 2011. Picoliter DNA sequencing chemistry on an electrowetting-based digital microfluidic platform. Biotechnol. J. 6 (2), 165–176.
Wheeler, A.R., Moon, H., Kim, C.C., Loo, J.A., Garrell, R.L., 2004. Electrowetting-based microfluidics for analysis of peptides and proteins by matrix-assisted laser. desorption/ionization mass spectrometry. Anal. Chem. 76 (16), 4833–4838.
Zhou, J., Lu, L., Byrapogu, K., Wootton, D.M., Lelkes, P.I., Fair, R., 2007. Electrowetting-based multi-microfluidics array printing of high resolution tissue construct with embedded cells and growth factors. Virtual Phys. Prototyp. 2 (4), 217–223.